JTTEE5 16:783–790
DOI: 10.1007/s11666-007-9077-9
1059-9630/$19.00 © ASM International

Optimization of a Rotating Twin Wire-Arc Spray Gun

Rodolphe Bolot, Hanlin Liao, Crisalia Mateus, Christian Coddet, and Jean-Michel Bordes

(Submitted March 6, 2007; in revised form June 7, 2007)

This paper presents a CFD (Computational Fluid Dynamic) study and experimental results concerning a rotating twin wire-arc spray process for the production of coatings on engine cylinder bores. In this process, the wire atomization is performed using a gas injection coaxially with the cylinder axis. The thermal spray tool is equipped with a deviation head rotating around the cylinder axis and allowing deflecting the droplet spray perpendicularly to the cylinder surface. The initial deviation head was found to be not sufficiently efficient so that a new deviation head incorporating an inclined slot was designed and used. Both CFD results and experiments showed that this new deviation head is more efficient. Moreover, it allowed increasing the coating bond-strength up to the specifications imposed by PSA Peugeot-Citroen. The present article shows that the wire-arc spray technology may replace efficiently the Atmospheric Plasma Spray (APS) for the thermal spray of coatings on engine cylinder bores. Moreover, it shows how CFD may help in solving industrial problems. In particular, the FLUENT CFD code was used in order to perform improvements of the deviation head design.

Keywords computational fluid dynamics, internal thermal spray, twin wire-arc

1. Introduction

The replacement of cast iron sleeves through thermal spray coatings is an interesting alternative to improve the inter-bore reliability, to reduce weight and to reduce the inter-bore distance for automotive engines. Most of the actual production and pilot equipments use the ROTAPLASMA (Ref 1-5) process to provide such functional coatings. However, the wire-arc spray process may often present different advantages like a higher deposition rate and a lower cost of the produced coatings. The LDS (Lichtbogendrahtspritzen) technology (Ref 6) developed by DaimlerChrysler is a wire-arc process working with two wires, whereas the PTWA (Plasma Transferred Wire Arc) process (Ref 7-8) designed by Flame Spray Industries and Ford Motor Company use a single wire.

This article was originally published in *Global Coating Solutions, Proceedings of the 2007 International Thermal Spray Conference*, Beijing, China, May 14-16, 2007, Basil R. Marple, Margaret M. Hyland, Yuk-Chiu Lau, Chang-Jiu Li, Rogerio S. Lima, and Ghislain Montavon, Ed., ASM International, Materials Park, 2007.

Rodolphe Bolot, Hanlin Liao, Crisalia Mateus, and **Christian Coddet**, LERMPS, University of Technology of Belfort-Montbéliard, Site de Sévenans, Belfort, 90010, France; and **Jean-Michel Bordes**, PSA Peugeot Citroën, Belchamp Technical Center, Voujeaucourt, France. Contact e-mail: rodolphe.bolot@utbm.fr.

The twin wire-arc spray process allows elaborating quite low-cost metallic coatings. A twin wire-arc spray gun is composed of two consumable electrodes (i.e., two metallic wires) guided toward a converging point wherein an electric arc is generated, thus permitting the melting of the continuously advancing wires. An atomizing gas flowing through the arc ball region permits to produce a molten droplet spray jet that is directed toward the surface of the part to be coated. The present study concerns the development of a thermal spray process for the coating of engine cylinder bores wherein a deviation device rotates around the arc ball formed by two consumable wires.

Several solution techniques were proposed in the literature for this type of process:

- The first method (TAFA Inc., 1999) (Ref 9) consists in atomizing the wire-ends with a primary gas injected coaxially with the rotation axis (i.e., parallel to the access direction and to the wires as well). In this case a secondary flow issuing from a deviation device is used to deflect the molten droplet spray perpendicularly to the cylinder surface. One may thus expect small differences in the wire-ends atomization at different rotation angles and use a device wherein only the deviation head rotates around the wires.
- The second one (Sulzer-Metco, 2000) consists in a direct atomization of the wire-ends using a gas flow injected perpendicularly to the rotation axis (Ref 10). Thus, a primary gas issuing from a cross-shaped orifice is blown on the arc ball and a secondary gas is injected through a set of cylindrical holes distributed along a circular line centered about the primary orifice. The secondary gas allows a constriction of the metallic droplet spray stream to reduce overspray. However, the atomizing process depends on the relative angle between the atomizing gas direction and the wire plan orientation so that the whole

spray device must rotate in order to keep this angle (e.g., perpendicular to the wire plan) and avoid strong variations of the coating thickness distribution.

– The third one (DaimlerChrysler, 2003) includes a system for incurving the wires at 90° before their atomization (Ref 6). Thus, the atomizing gas may be injected perpendicularly to the surface to be coated so that there is no need for a secondary gas. However, the whole spray device must also rotate according to this method.

Figure 1 presents a schematic view of the two first solution techniques described above. In Fig. 1a, the primary orifice is a cross and the secondary gas issues from eight equally spaced holes with a 1.6 mm diameter. All orifices are connected with the pressurized interior chamber.

The thermal spray device used in the present study was based on the first solution technique described above (Fig. 1b). A TAFA 9000 gun (from TAFA Inc., Concord, NH, USA) equipped with an extension with a 44 mm outside diameter was used. The only part of the gun that rotates is a crown (shown in Fig. 1b only) over which the deviation device is fixed. Thus the central part (brown color) of the device and the wires do not rotate. The present design of the deviation head is based on the TAFA 939ID extension (Ref 9) that is composed of three lines of drilled holes presenting a semicircular distribution.

Some preliminary results obtained under nonrotating conditions with the TAFA 939ID head tended to indicate that the deviation function was not fully satisfying (Ref 11). Thus, the initial deviation device that was first tested in the present study was quite similar to that shown in Fig. 1b, except that it contains more holes (40 instead of 31). This modification was operated in order to increase the deviation air flow rate obtained for a given feeding pressure, thus reinforcing the deviation function. This first device is shown in Fig. 2. It presents three lines of drilled holes distributed on three different radiuses. The first line is composed of 10 holes, whereas the two others include 15 ones. The two shoulders allow screwing the head in the rotating crown.

2. Experimental Results

Some experiments were conducted using type 38T wires (98% iron (Fe), 1.6 mm diameter) provided by TAFA. Two different types of samples were used:

– Steel cylinders (10 mm thick with a 25 mm diameter) for adhesion tests.
– 2 mm thick rectangular samples for microstructures analysis, porosity level, oxide content, and hardness measurements.

All samples were degreased and sandblasted providing a roughness Ra of 4-5 μm.

2.1 Coating Specifications

Barbezat (Ref 5) pointed out that the coating adhesion is the main key factor for the success of thermal spray on engine cylinder bores and estimation shows that the necessary adhesion is about 15 MPa (although a value of 30 MPa is preferred).

The coating specifications provided by PSA Peugeot Citroen were the following ones: a coating micro-hardness (HV0.3) not smaller than 220 (but not too high in order to remain machinable), a coating porosity level of 2 or 3% (at least not exceeding 5%), a bond strength higher than 20 MPa and a coating thickness of 300-400 μm (as-sprayed) and 200 μm after machining. Moreover, the residual stress level in the coating must remain very low or in a compressive state, the coating has to resist to the high temperatures (surface temperature of about 150°C at the top of the cylinder for an aluminum block) and to thermal chocks (more particularly at the engine start). It must also

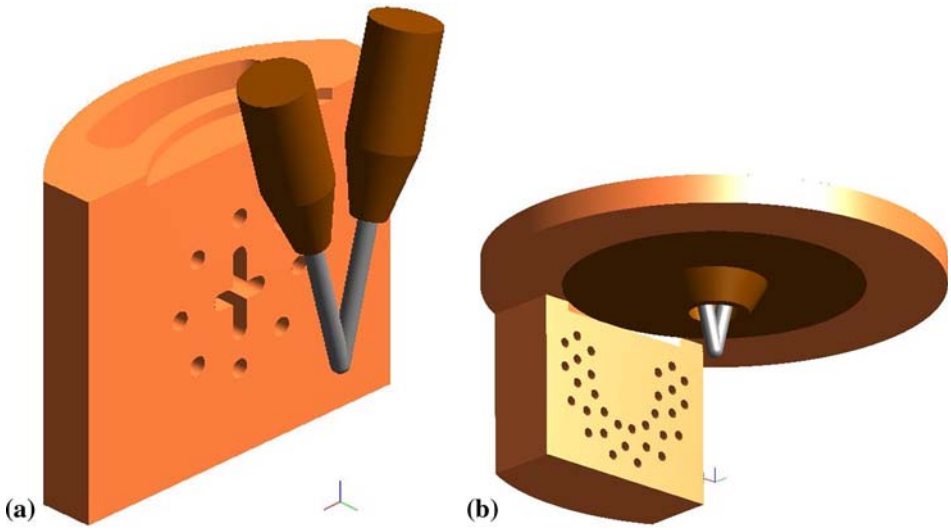

Fig. 1 Schematic view of two solution techniques: (a) perpendicular atomization with a cross-shaped orifice (Ref 10) (b) vertical atomization used in conjunction with a deviation device consisting in a set of 31 holes presenting a U-shaped distribution (Ref 9)

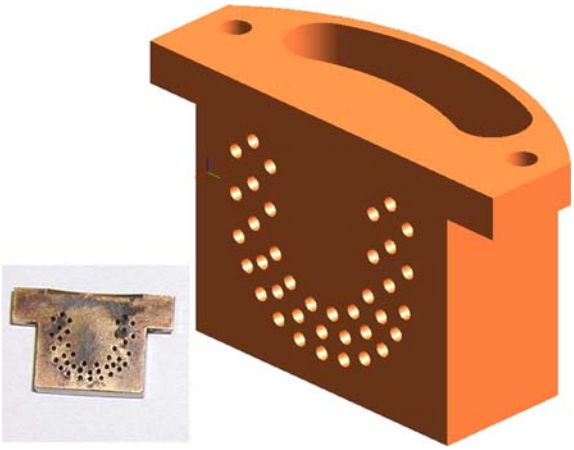

Fig. 2 First deviation head tested in the present study

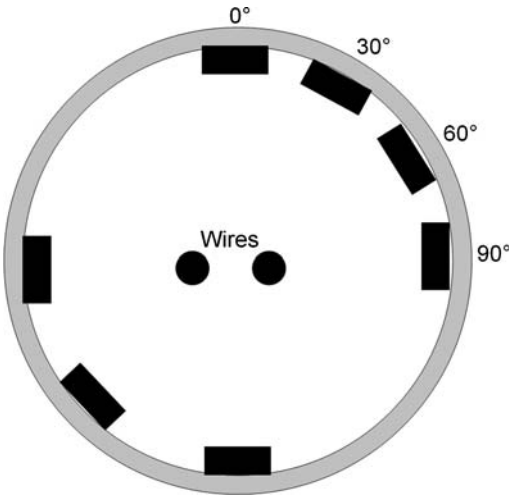

Fig. 3 Sample distribution in the cylinder

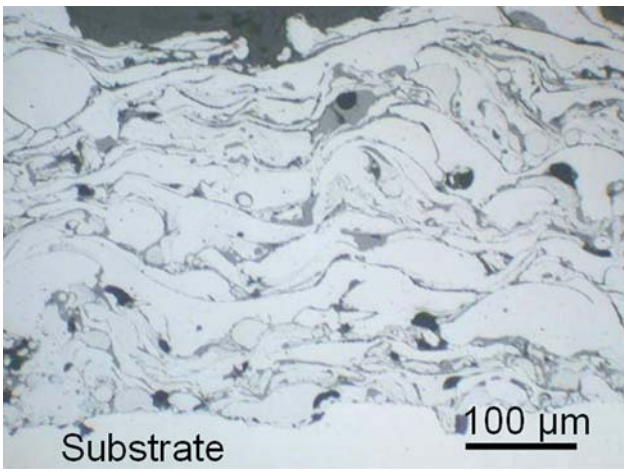

Fig. 4 Typical macrostructure of a coating produced using a rotating twin wire-arc spray gun

resist to the corrosive environment and present good tribological properties.

2.2 Elaborating Conditions

The samples were placed in a cylinder in order to check the matter distribution homogeneity for different angles as shown in Fig. 3. The torch was moved axially in the cylinder with a vertical displacement velocity of 40 mm/s and a rotational speed of 120 rpm. The electric arc current intensity was 150 A and the voltage ranged between 30 and 35 V.

Two different atomizing gas pressures (P_{ato}) of 0.4 and 0.6 MPa were considered and the deviation air flow rate was adjusted at 80, 90, and 100 standard cubic meters per hour (sm^3/h hereafter) respectively, except for experiments performed at $P_{ato} = 0.6$ MPa for which only the highest value of the deviation gas flow rate was used (i.e., 100 sm^3/h).

The coating thickness, porosity level, and oxide content measurements were obtained by image analysis. Although, this method is not sufficiently accurate for a quantitative analysis, it is perfectly suitable for a comparative study. Ten different pictures randomly generated were used for each condition and the results were averaged. Figure 4 presents the typical structure of the coating including overlapping lamellae, oxides, and different size pores as well.

2.3 Summary of Experimental Results

The objective of the present article is not to provide an exhaustive list of experimental data. Thus, Table 1 summarizes the main results. Experimental results showed that the measured coating thickness (around 400 µm) was only weakly sensitive to the increase in the deviation gas flow rate but an increase in the coating thickness was observed with the increase in the atomizing pressure (+10% at 0.6 MPa versus 0.4 MPa). At the lowest atomizing pressure of 0.4 MPa, the thickness distribution at the different spray angles showed a maximum difference of about 13% for deviation gas flow rates higher than 80 sm^3/h. However, this maximum difference was dramatically increased at 0.6 MPa. In particular the coating thickness is the lowest at 0° and the highest at 60° (+75%). This significant difference represents an important drawback.

The coating roughness was found to increase somewhat with the deviation gas flow rate (e.g., *Ra* from 17 to 26 µm at the 0° angle, and *Ry* from 160 to 190 µm).

The porosity level determined by image analysis is homogeneous versus the parameters. In particular, it was always lower than 3% whatever the parameters and presented a mean value of about 2.2%. The slight decrease in the porosity level with the increase in the deviation gas flow rate was certainly provided by an increase is the mean droplet velocity prior to their impact on the substrate. Moreover, according to Barbezat (Ref 2), this range of the residual porosity level is ideal because it permits to keep some lubricant in the micro-cavities.

Table 1 Summary of the main experimental results

P_{ato}, bars	4			6
$Q_{deviation}$, sm^3/h	80	90	100	100
Coating thickness, μm	380	385	395	435
Maximum difference, μm	80	40	50	255
Roughness *Ra*, μm	19	23	28	30
Roughness *Ry*, μm	180	180	205	225
Porosity level, %	2.3	2.2	2	2.3
Oxide content, %	8	6	5	5
Hardness $HK_{300\ g}$	350	280	310	290
Bond strength, MPa	6	9	9	12

The oxide level presents a decreasing tendency with the increase in the deviation gas flow rate (decrease from 8% to 5% for 80 and 100 sm^3/h, respectively). This decrease was certainly provided by a lower time of flight of the droplets due to the increase in their velocity.

Micro-hardness measurements obtained using Knoop indentation with a load of 300 g for 15 s showed homogenous results for the different angles and parameters ($HK_{300\ g}$ of about 300) and a corresponding value of 6 GPa was deduced for the Young Modulus determined according to (Ref 12). The weakly decreasing tendency obtained for the coating hardness with the increase in the deviation gas flow rate is also certainly linked to the decrease in the coating oxide content.

Bond strength measurements performed according to ASTM C633-79 standard using an adhesive film from Cytec Fiberite (FM1000) present an increasing tendency (from 6 to 9 MPa) while the deviation gas flow rate is increased from 80 to 100 sm^3/h. This increase was certainly provided by a higher mean droplet velocity prior to their impact, thus reinforcing the mechanical bonding. Moreover, an increase was also obtained while the atomizing pressure was increased to 0.6 MPa (12 MPa in this case). This increase could be explained by a decrease in the droplet size (and subsequent increase in their velocity) with the increase in the atomizing gas pressure and flow rate. However, all these values are rather low and especially below the coating specifications.

From the measurement of the spray pattern positioning without any vertical displacement of the gun, it was noticed that the deviation head was not efficient enough, providing a spread spray stream. A spread spray stream may result in cooling fringe droplets and affect the coating quality. Thus, Computational Fluid Dynamics (CFD) was used to improve the deviation function of the gun and provide a more constricted spray.

3. Modeling Results

To make a process design and development robust, it is important that the correlation between the gun operating parameters and the resulting in-flight particle characteristics is well understood and predictable (Ref 13). Considering that the deviation head design is certainly the most important parameter for the present application, it is thus important to understand how this parameter acts on in-flight particle characteristics.

The goal of the present CFD study was to test different deviation head design in order to satisfy the following objectives:

- improve the deviation function and provide a narrowing of droplet spray in order to limit overspray and improve the coating quality,
- offset some other defects sometimes detected such as a particle stacking on the central part of the deviation head, and to
- improve the coating adhesion mainly.

These objectives must be achieved without providing other drawbacks such as a perturbation of the electric arc.

All the following results concern the modeling of the flow for different deviation heads. The FLUENT CFD software package (FLUENT Inc., Lebanon, NH, US) was used for the computations (6.2.16 release). FLUENT has been a leader in the development of CFDs for over 20 years. Its extensive range of multiphysics capabilities makes it one of the most comprehensive software tools available to the CFD users. In FLUENT, unstructured grid technology is used meaning that it can consist of elements in a variety of shapes such as hexahedrons, tetrahedrons, prisms, or pyramids (for 3D cases). These elements are created using automated controls in GAMBIT, the FLUENT preprocessor. Moreover, FLUENT is based on a finite volume approach and incorporates both segregated and coupled solvers.

It the present case, it was used to compute the flow through different deviation heads of the wire-arc spray gun.

The considered parameters were:

- a deviation gas flow rate of 90 sm^3/h.
- an atomizing gas flow rate of 14 sm^3/h (i.e., atomizing gas pressure of 0.4 MPa).

In fact, the atomizing gas pressure mentioned in the first part of the study is the feeding pressure but the atomizing gas flows through a four meter long flexible duct before being discharged. Thus, the corresponding gas flow rates were calculated for different feeding pressures in the range from 0.2 to 0.6 MPa. As a first approximation, a linear fitting was derived so that the atomizing gas flow rate was estimated from:

$$Q_v(\mathrm{sm^3/h}) = 34.2\ P_{\mathrm{ato}}(\mathrm{MPa})$$

GAMBIT was used to build the CAD geometry of Fig. 2. The crown over which the deviation head is fixed was then generated and the wires as well. The atomizing nozzle was formed of two inversed conical parts (see Fig. 5 for example) and its throat diameter was 6 mm. Once these parts were generated, a cylinder was added and all the solid parts were subtracted from this cylinder using a Boolean operation. In the present case, the cylinder was 50 mm high with a diameter of 70 mm.

Within FLUENT, the ideal gas option was selected for the density formulae and the standard k-ε turbulence model was activated. The segregated solver was activated because it is perfectly suitable for the present type of applications. Moreover, the SIMPLEC pressure-velocity coupling algorithm was preferred to SIMPLE because it allows using a higher under-relaxation factor for the pressure correction equation (e.g., such as 0.9 instead of 0.3), thus allowing a faster convergence. Moreover, the differences between results obtained with first order and second order accurate schemes (for the discretization of the convective term of the solved variables) were not significant.

The initial conditions were zero velocity components and zero relative pressure everywhere in the domain. Moreover the initial temperature was set to 288 K and the turbulence kinetic energy and its dissipation rate were initialized in order to provide low values of the turbulent viscosity (such as $k_{ini} = 10^{-3}$ m^2 s^{-2} and $\varepsilon_{ini} = 10$ m^2 s^{-3}). This method allows avoiding large transient increase of the pressure in the internal chamber that could be detrimental to the calculation convergence under the present conditions.

For the boundary conditions, two different inlet regions were created for the atomizing and deviation gases and two different pressure outlets were created for the top annular section (free space between the cylinder wall and the cylindrical gun extension) and the circular bottom, respectively. The inflow boundary conditions were specified by imposing a mass flow rate on each inlet and by specifying a turbulence intensity of 5% and the hydraulic diameter of the orifices. With this method, the turbulence kinetic energy and its dissipation rate are thus calculated from $k = 3/2*(0.05*V)^2$ and $\varepsilon = 2.35*k^{1.5}/D_H$ in which V is the mean flow velocity over the boundary and D_H is the hydraulic diameter of the considered orifice.

A zero relative pressure boundary condition was applied at the free limits of the domain with a temperature of 288 K for the incoming fluid and a turbulence intensity of 5% as well.

All other surfaces were solid walls but were considered as different regions such as the lateral face of the cylinder or the wire-ends for example, thus enabling to consider different boundary condition types for these faces.

3.1 Initial Deviation Head of Fig. 2

This first case was performed with a grid containing a little more than 0.3 Million of cells (tetrahedrons only). Figure 5 presents the pressure field in the symmetry plan of the initial deviation head of Fig. 2. The maximum pressure (a little less than 0.5 MPa) is found in the deviation gas feeding chamber that presents an extruded bean shape in 3D (as shown in Fig. 2 for example). The pressure drops through the different holes (total number of 40 as shown in Fig. 2) connecting the chamber to the external environment.

Figure 6 presents the velocity vectors in the same symmetry plan. The maximum velocity is found at the exit of the holes connecting the internal chamber to the external environment. According to the model, the flow is slightly supersonic at the exit of these holes.

Figure 7 presents the droplets trajectories for the initial deviation head design. The stream color was given for the particle velocity. The droplet size was set according to a Rosin-Rammler distribution (Ref 14) with a minimum droplet size of 30 μm, a maximum size of 100 μm and a mean size of 50 μm. For this distribution, the mass fraction $y(d)$ of particles with a size greater than d is given by:

$$y(d) = \exp\left[-\left(\frac{d}{\bar{d}}\right)^n\right]$$

where $\bar{d}$ was set to 50 μm and n, the spreading parameter was set to 3.

This droplet size distribution was that intuitively assumed for the deviation head design optimization. Later measurements based on particle collecting were however in accordance with the present choice ($\bar{d}$ parameter of 45 μm and $n \approx 2.8$ for the present deviation head).

One may notice that the droplet stream deviation is not sufficient for this case. The center of the droplet flux at the impact point on the cylinder surface is found to be about

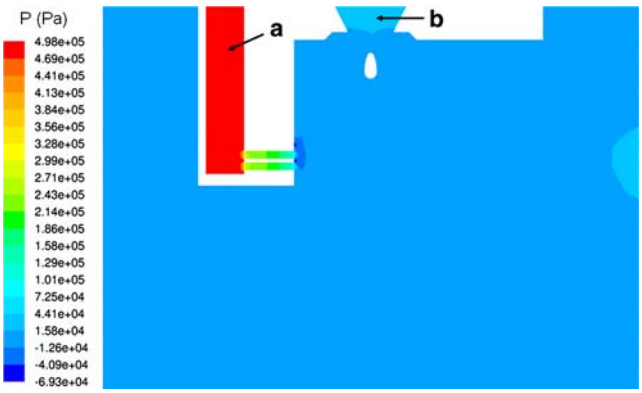

Fig. 5 Pressure field in the symmetry plan for the initial head design (40 holes) (a) deviation gas feeding chamber, (b) atomizing nozzle

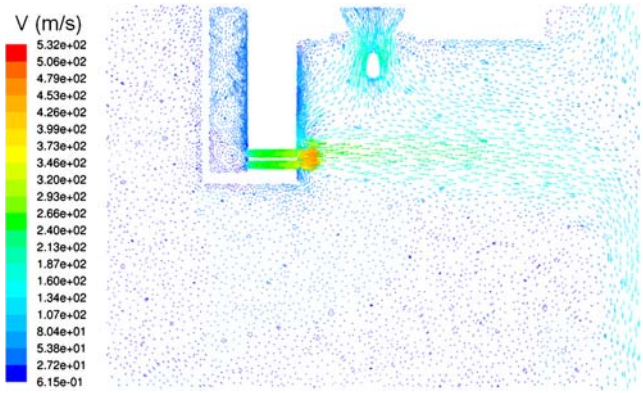

Fig. 6 Velocity vectors in the symmetry plan for the initial gun design

20 mm below the deviation head lowest holes. This is a little too down in comparison with experimental results obtained under nontranslating conditions (i.e., fixed vertical position of the gun).

3.2 Improvement of the Deviation Head Design

Different types of deviation heads were tested. Some of them enabled some improvements from both the modeling point of view and the experimental point of view. However, a perturbation of the electric arc was sometimes noticed. Finally, one of them retained our attention. This head design was specially intended to provide a narrowing of the droplet jet in the vertical direction. It is composed of an inclined slot (15° inclination) with vertical lines of holes as shown in Fig. 8. Moreover, three holes were added on the top part of the head in order to prevent any particle stacking on the head surface. The effect of these holes was not sufficient to perturb the electric arc but they were found to offset the effect of the low-pressure region observed between the atomizing and deviation gases, which was intuitively considered as responsible for the particle stacking on the gun head.

The inclined slot is 1.5 mm thick and 14 mm wide. Moreover, 18 holes drilled horizontally allow a constriction of the droplet jet in the transverse direction. The overall cross-section connecting the interior chamber to the environment is more important for this new head in comparison with the old one (i.e., 36.8 mm^2 instead of 31.4 mm^2).

Figure 9 presents the pressure field in the symmetry plan for the above head design. Although the deviation gas flow rate was the same as that used previously (i.e., 90 sm^3/h), the corresponding pressure in the deviation gas chamber is about 0.1 MPa lower because of the higher overall cross-section of the holes connecting the chamber to the environment.

Figure 10 presents the computed velocity vectors in the same symmetry plan. For the reasons mentioned above, the maximum velocity is somewhat lower in comparison with that obtained for the initial design. However, the jet issuing from the slot presents a longer core in comparison with those issuing from the circular holes of the first

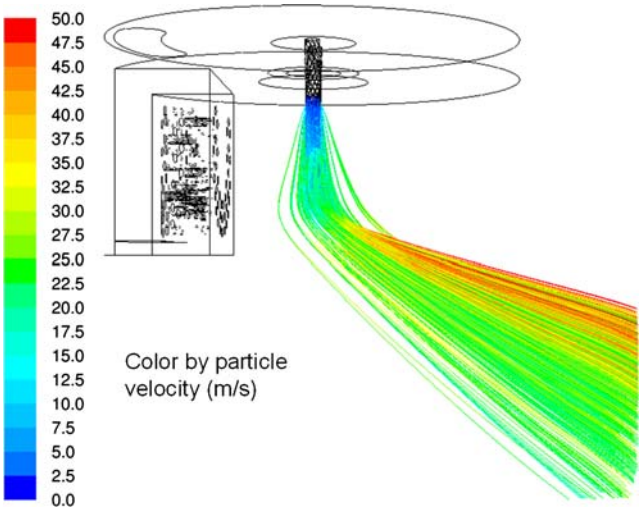

Fig. 7 Droplet deviation for the initial head design

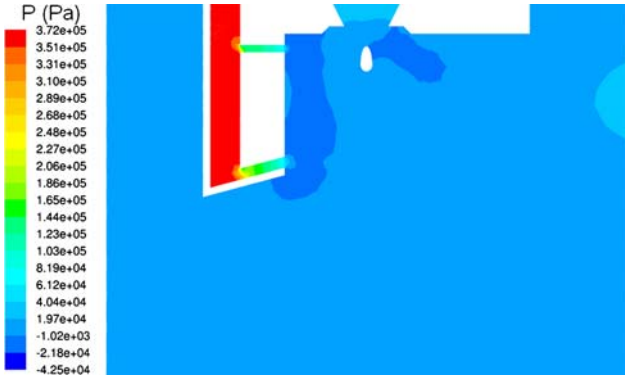

Fig. 9 Pressure field in the symmetry plan computed for the new head design

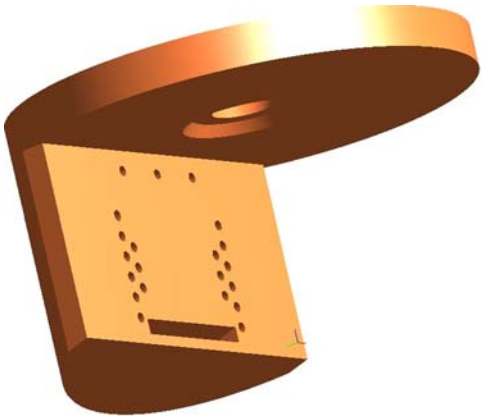

Fig. 8 Gun design composed of an inclined slot and vertical lines of holes

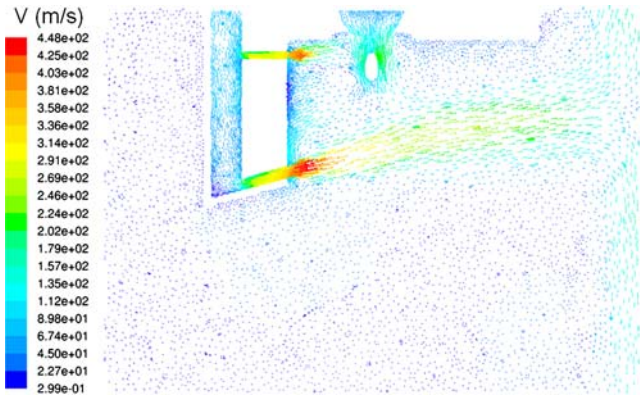

Fig. 10 Velocity vectors in the symmetry plan for the new head design

deviation head. Meanwhile, the use of the standard k-ε turbulence model is certainly not favorable to the deviation head composed of circular holes because this model is particularly known for underestimating the length of the core of round jets.

Figure 11 presents the droplet stream deviation for the same size distribution as that of Fig. 7. One may notice that the maximum droplet velocity obtained for this new design is almost 20 m/s higher than that showed in Fig. 7 and a similar difference was found for the mean velocity that was increased by about 50%. Moreover, the droplet stream deviation is much more efficient for the present new design. In particular, the vertical positioning of the droplet flux center is almost aligned with the inclined slot at the spray distance and the droplet impact angle is approximately perpendicular to the surface to be coated (i.e., horizontal droplet stream). Moreover, measurements of the particle size distribution (based on collected particles) indicate that the mean droplet size is smaller for this new design of the deviation head in comparison with that measured for the initial design. This result tends to indicate that the droplet flux could be even more deviated because the smallest particles are more easily entrained. It also confirms that a secondary atomization takes place where the droplets interact with the deviation gas because otherwise the size distribution would be almost identical for the two deviation heads. Finally, because of the smaller droplet size mentioned above, it is obvious that the differences obtained with the two different deviation heads are still reinforced. In particular the difference in the droplet velocity would be still greater if two different droplet size distributions had been considered for the two deviation heads.

The interest in using this new head design was mentioned in (Ref 15). In addition to the just mentioned advantages, the new design was found to provide a narrowing of the droplet size distribution and a significant improvement of the bond strength that was increased to 22 MPa instead of about 10 MPa for the initial design. This value of the bond strength is now sufficient for the present application. In particular, it is higher than that obtained from the LDS and PTWA technologies used without special pretreatment methods (about 15 MPa). Moreover, advanced surface preparation processes such as high pressure water jetting (Ref 7-8) could allow the bond strength values to increase up to 40 MPa or more if necessary.

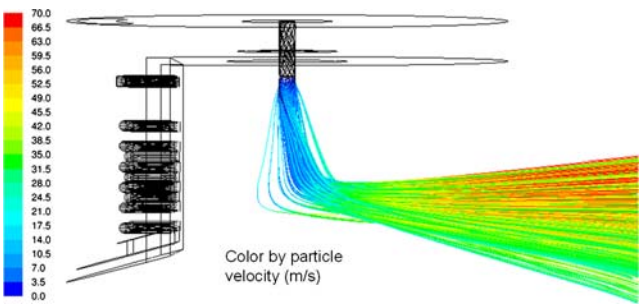

Fig. 11 Droplet stream deviation obtained with the new design

4. Conclusion

The present study was devoted to improve the design of the gun head used for the rotating twin wire-arc spray process. The initial design based on the TAFA 939ID extension was presented but the corresponding experiments showed a low adhesion of the produced coatings. CFD results computed with FLUENT tended to demonstrate that the deviation of the droplet stream was not sufficient for this initial design. Thus, a modified head design was generated in order to improve the deviation function and provide a constriction of the droplet spray jet. It was shown that the new design allows increasing the droplet velocity by about 20 m/s for the same droplet size distribution. Moreover, a narrowing of the droplet size distribution was observed experimentally. The new head design allowed increasing the coating bond strength that was twice higher in comparison with the reference case. This higher adhesion was provided by an improvement of the droplet impact angle on the surface to be coated, by the constriction of the droplet stream, by a narrowing of droplet size distribution and by a higher droplet mean velocity. The present twin wire-arc process developed at LERMPS presents several advantages: the process stability is improved and the cost is lower in comparison with APS. Moreover, because only the deviation head rotates, it is simpler to implement in comparison with some other wire-arc processes involving a rotation of the whole thermal spray gun.

References

1. G. Barbezat, The State of the Art of the Internal Plasma Spraying on Cylinder Bore in AlSi Cast Alloys, *Int. J. Automot. Technol.*, 2001, **2**(2), p 47-52
2. G. Barbezat, Advanced Thermal spray Technology and Coating for Lightweight Engine Blocks for the Automotive Industry, *Surf. Coat. Technol.*, 2005, **200**, p 1990-1993
3. G. Barbezat, High Performance Coatings Produced by Internal Plasma Spraying on Engine Blocks of New Generation, *Thermal Spray Solutions: Advances in Technology and Application*, DVS, Düsseldorf, Germany, 2004. ISBN: 3-87155-792-7
4. G. Barbezat, Coating Deposition of Bearing Materials on Connecting Rod by Thermal Spraying, *Thermal Spray Connects: Explore its Surfacing Potential!* E. Lugscheider, Ed., DVS, Düsseldorf, Germany, 2005, 1574+ pages. ISBN: 3-87155-793-5
5. G. Barbezat, Importance of Surface Preparation Technology Prior to Coating Deposition on Cylinder Bores for High Performance Engines, *Thermal Spray 2007: Global Coating Solutions*, B.R. Marple, M.M. Hyland, Y.-C. Lau, C.-J. Li, R.S. Lima, and G. Montavon, Eds., ASM International, Materials Park, OH, USA, 2007
6. D. Nowotni, C. Wanke, T. Haug, and P. Izquierdo, ''Inner Torch,'' US Patent 6,667,460 B2, 2003
7. K. Bobzin, E. Lugscheider, F. Ernst, J. Zwick, T. Schlaefer, C. Verpoort, A. Schwenk, F. Schreiber, T. Wenz, D. Cook, K. Kowalsky, and J. Conti, Coating Bores of Light Metal Crankcases, *Building on 100 Years of Success*, B.R. Marple, M.M. Hyland, Y.C. Lau, R.S. Lima, and J. Voyer, Eds., ASM International, Materials Park, OH, USA, 2006

8. E. Lugscheider, R. Dicks, K. Kowalsky, D. Cook, K. Nassenstein, and C. Verpoort, A Materials System and Method of its Application for the Wear Protection of Aluminium Engine Cylinder Bore Surfaces, *Thermal Spray Solutions: Advances in Technology and Application*, DVS, Düsseldorf, Germany, 2004. ISBN: 3-87155-792-7
9. J.P. Dunkerley, T.A. Friedrich, and G. Irons, ''Apparatus for Rotary Spraying a Metallic Coating,'' US Patent 5,908,670, 1999
10. R. Benary, Arc Thermal Spray Gun Extension and Gas Jet Member Therefor,'' US Patent 6,091,042, 2000
11. M. Boulais Monin, Etude Paramétrique et Caractérisation de Matériaux Obtenus par Projection Thermique: Application à l'Evolution des Moteurs d'Automobiles, Thesis, University of Franche-Comté, 1998 (in French)
12. D.B. Marshall, T. Noma, and A.G. Evans, A Simple Method for Determining Elastic-Modulus-to-Hardness Ratio Using Knoop Indentation Measurements, *J. Am. Ceram. Soc.*, 1982, **65**(10), p C175-C176
13. J. Stanisic, D. Kosikowski, and P.S. Mohanty, High-Speed Visualization and Plume Characterization of the Hybrid Spray Process, *J. Therm. Spray Technol.*, 2006, **15**(4), p 750-758
14. K.M. Djamarani and I.M. Clark, Characterization of Particle Size Based on Fine and Coarse Fractions, *Powder Technol.*, 1997, **93**, p 101-108
15. C. Coddet, R. Bolot, J.M. Bordes, and C. Meekel, Dispositif de Projection de Particules Métalliques par Arc Electrique Entre Deux Fils, FR Patent 2 866 901, French Registration Number 04 02049, 2005 (in French)